Colloid Polym Sci (2017) 295:995–1006
DOI 10.1007/s00396-017-4049-1

ORIGINAL CONTRIBUTION

Synthesis of amphiphilic block copolymers containing ferrocene–boronic acid and their micellization, redox-responsive properties and glucose sensing

Muhammad Saleem[1] · Li Wang[1] · Haojie Yu[1] · Zain-ul-Abdin[1] · Muhammad Akram[1] · Raja Summe Ullah[1]

Received: 3 December 2016 / Revised: 1 February 2017 / Accepted: 12 February 2017 / Published online: 22 April 2017

Abstract Amphiphilic block copolymer PMAEFc-*b*-PMVAPBA was synthesized by reversible addition–fragmentation chain transfer (RAFT) polymerization. The hydrophobic and hydrophilic blocks of copolymers self-assembled into spherical micelles in aqueous solution. The redox behaviour of ferrocene was studied by using water-soluble $(NH_4)_2Ce(NO_3)_6$ and $NaHSO_3$ as the oxidizing agent and reducing agent, respectively. The change in polarity and swelling of micelles increased the hydrodynamic diameter due to the oxidation of ferrocene, while glucose binding with boronic acid hydroxyls leads to unimers or smaller aggregates. TEM and DLS were used to investigate the redox-controlled behaviour of micelles. This redox-responsive behaviour would provide a prerequisite for detection/binding of biological analytes study and redox-controlled release of drug.

Keywords Ferrocene · Boronic acid · Redox responsive · Micelles · Amphiphilic

Introduction

The introduction of different functional groups into the polymer greatly enhances its practical applications in biodiagnosis, separation media and therapeutics [1–3]. The selection of monomers depends on their intended applications. Amphiphilic block copolymers have attracted significant attraction due to their self-assembly in selective solvents to form vesicles or micelles based on the solubility of their hydrophilic and hydrophobic segments [4, 5]. Among them, stimuli-responsive polymers have been in the focus of intensive research in the last decade. The vast majority of reports deal with temperature, light and pH changes as external triggers. In recent years, the redox stimulus has gained significant attention for switching polymer conformation or the polarity of surfaces. The introduction of ferrocene moiety into polymers has been extensively used for the construction of redox stimuli-responsive polymers owing to reversible oxidation and reduction of ferrocene units by electrochemical and chemical means [6–8]. Ferrocene-containing block copolymers self-assemble and may induce change in polarity of ferrocene-bearing blocks due to reversible redox reactions. Thereby, these block copolymers form micelles with redox-triggered activity, which are particularly useful for potential applications of redox-regulated release of encapsulants [9–12].

Controlled radical polymerization (CRP) is generally utilized for the synthesis of block copolymers with tuneable molecular weight and chemical composition and greater freedom to design new and controllable micelles [13]. Among CRP techniques, reversible addition–fragmentation chain transfer (RAFT) polymerization is the most versatile technique and used for the synthesis of well-defined functional polymers with controlled molecular weight distributions and narrow PDI. Typically, RAFT offers the advantages of conventional free radical polymerization and requires milder reaction conditions than ionic polymerization [1, 14–17]. Polymers with boronic acid (BA) groups are versatile, especially for saccharide sensing applications. BA recognizes *cis*-diol configuration of saccharides through reversible covalent complex

✉ Li Wang
opl_wl@dial.zju.edu.cn

✉ Haojie Yu
hjyu@zju.edu.cn

[1] State Key Laboratory of Chemical Engineering, College of Chemical and Biological Engineering, Zhejiang University, Hangzhou 310027, China

formation in aqueous solution, and thus, it represents an ideal synthetic molecular receptor and can be utilized for sensing biologically related molecules including proteins, peptides, drugs and enzymes [18, 19]. Among redox-responsive metallopolymers, ferrocene is widely used due to its fascinating reversible redox chemistry. Redox-responsive ferrocene with boronic acids can operate in two different ways in glucose application as through electrochemical signal translation of binding event of saccharides with boronic acid hydroxyls by cyclic voltammetry. Secondly, ferrocene-containing block copolymers self-assemble and may induce change in polarity of ferrocene-bearing blocks due to reversible redox reactions. Thereby, these block copolymers form micelles with redox-triggered activity, which are particularly useful for potential applications of redox-regulated release of encapsulants.

In this article, we have chosen a second approach and synthesized novel block copolymer of ferrocene-containing boronic acids and investigate the redox-controlled behaviour of micelles. The covalent attachment of boronic acids with biomolecules can provide the opportunity to develop novel materials with the integrated properties of both systems (redox-responsive ferrocene and boronic acids for binding diols) for several applications such as biotechnology, nanotechnology, medicine and especially saccharide sensing. In addition, change in redox behaviour could trigger an electrochemical stimulus on binding of diols with boronic acids. Furthermore, the self-assembly of the biomolecule and block copolymer may also form redox-responsive micelles, which can exhibit redox-triggered response by the change in their shape or size. Xiao et al. reported the synthesis of amphiphilic block copolymers with aldehyde and ferrocene containing hydrophobic block and explored their redox-responsive micellization behaviour [20].

Janczewski et al. reported the synthesis of poly(ferrocenyl silane) amphiphilic oligomer, which displayed redox active reversible properties and morphology transformation upon change in the redox state of ferrocene [11]. More recently, Liu et al. reported ferrocene-based block copolymer and explored its redox chemistry by assembling and disassembling of micelles for the release of dye and thus, it offered a system for redox controlled release of drugs [9]. Micelles morphology is more important than block copolymers, as micelles are widely used in industrial and biological fields for their ability to dissolve and move non polar substances through an aqueous medium or to carry drugs, which are often scarcely soluble in water. The carrying ability of micelles can be altered by changing the parameters, which determine their size and shape. In all aforementioned literature, ferrocene-based polymers have been synthesized and their redox chemistry was investigated. To the best of our knowledge, dual-responsive ferrocene-containing block copolymers have not yet been reported. Keeping these aforesaid findings and our interest to explore morphology of ferrocene boronic acid-based block copolymer through micellization, we reported the synthesis of ferrocene boronic acid-based amphiphilic block copolymer (PMAEFc-*b*-PMVAPBA) by using 2-methyl-2-[(dodeclsulfanyl thiocarbonyl) sulfanyl]propanoic acid (DDMAT) as RAFT agent and explored its redox-responsive chemistry of ferrocene along with glucose sensitivity of the boronic acid by micellization.

In this perspective, particular emphasis is given to develop well-defined micelles morphology by introducing hydrophilic RAFT agent (i.e. DDMAT) in the block copolymer structure. These micelles are expected to show well-defined morphology and better redox-responsive behaviour to investigate the effect of ferrocene redox chemistry on glucose binding by micellization. The synthesized amphiphilic block copolymer contains a hydrophilic DDMAT as macrochain transferring agent (CTA) linked to a hydrophobic blocks of redox-active ferrocene moiety and boronic acid. Redox-responsive micelles of amphiphilic block copolymer (PMAEFc-*b*-PMVAPBA) were prepared and characterized as potential candidates for glucose sensing. Dynamic light scattering (DLS) and transmission electron microscopy (TEM) were used to investigate the redox-controlled behaviour of the micelles.

Experimental section

Materials

Ferrocenecarboxylic acid was purchased from Energy Chemicals and used without further purification. Oxalyl chloride was purchased from Sinopharm Chemical Reagent Co., Ltd. and used without further purification. Acetonitrile (MeCN), dimethylformamide (DMF) and methanol anhydrous were purchased from Sinopharm Chemical Reagent Co., Ltd. and used after drying by using 4 Å-type molecular sieves. Triethylamine (TEA), dichloromethane CH_2Cl_2 and tetrahydrofuran (THF) were purchased from Sinopharm Chemical Reagent Co., Ltd. and used after drying over 4 Å-type molecular sieves followed by reflux system. 2-Methyl-2-[(dodecylsulfanylthiocarbonyl)sulfanyl]propanoic acid (DDMAT) was purchased from STREM Chemicals Incorporated China. Methyl vinylamino phenylboronic acid and 2-(methacryloyloxy)ethyl ferrocencarboxylate (MAEFc) were synthesized according to previously reported methods [21]. Azobisisobutyronitrile (AIBN) was purchased from J & K Scientific Ltd. and recrystallized three times in methanol before use. All other reagents were from commercial resources and used as received unless otherwise noted.

Synthesis and micellization of PMAEFc-*b*-PMVAPBA

Amphiphilic diblock copolymer (PMAEFc-*b*-PMVAPBA) was synthesized by using DDMAT as chain transferring agent,

PMAEFc as ferrocene-based macroinitiator and methyl vinylamino phenylboronic acid (MVAPBA) as boronic acid-based monomer. The detailed synthetic procedure is as follows.

Ferrocenemonocarbonyl chloride

Ferrocenemonocarbonyl chloride (FcCOCl) was prepared by using ferrocenecarboxylic acid and oxalyl chloride (as a chlorinating agent) in CH_2Cl_2 and employing pyridine as a catalyst. In typical procedure, 20.7140 g (83.92 mmol) of FcCOOH was dissolved in freshly distilled CH_2Cl_2 (150 mL) and stirred well under Ar atmosphere. Pyridine (14.50 mL) and oxalyl chloride (15.50 mL, 180.72 mmol) were added to the above solution. The resulting solution was then stirred for 30 min at room temperature and allowed to reflux for 5 h. The contents of the reaction flask were evaporated to dryness under reduced pressure by using liquid nitrogen, and then residue was extracted carefully with petroleum ether by using in situ filtration. FcCOCl was stored under Ar atmosphere for the next experiment.

2-(Methacryloyloxy)ethyl ferrocencarboxylate

MAEFc was synthesized with slight modification in the reported method [21]. FcCOCl (8.3776 g, 33.74 mmol), 2-hydroxyethyl methacrylate (3.5338 mL, 33.74 mmol) and pyridine (8 mL) were dissolved in freshly distilled THF (80 mL), and the resultant mixture was refluxed for 4 h. The content of the reaction flask was filtered and then filtrate was dried on rotary evaporator. The product was precipitated in cold water and then washed thrice with distilled water to obtained pure brownish solid. ^{1}H NMR (600 MHz, $CDCl_3$) δ ppm: 6.22 (1H, Vinyl CH), 5.60 (1H, Vinyl CH), 4.75 (2H, Cp), 4.45 (4H, OCH_2CH_2O), 4.40 (2H, Cp), 4.25 (5H, Cp) and 2.00 (3H, CH_3).

Methyl vinylamino phenylboronic acid

MVAPBA was synthesized according to previously published report [22]. Typically, APBA (3.0 g, 0.020 mol) was dissolved in a round bottom flask containing a 1:1 mixture of THF and water (30 mL each). Sodium hydrogen carbonate (3.70 g, 0.044 mol) and methyl acryloyl chloride (4.59 g, 0.044 mol) were added to the flask at 0–5 °C. The solution was stirred for 5 h, and solvent was evaporated under reduced pressure. A solid crude product was obtained, which was further stirred in ethyl acetate (50 mL) for 2 h. The solution was filtered, and the ethyl acetate layer was washed with water, saturated sodium bicarbonate ($NaHCO_3$) solution, water and brine (40 mL of each solution). The ethyl acetate layer was concentrated on rotary evaporator providing the white solid. The monomer was purified by recrystallization three times in hot water. ^{1}H NMR (600 MHz, DMSO) δ ppm: 9.75 (1H, NH), 8.05 (2H, $B(OH)_2$), 7.90, 7.83–7.81, 7.50–7.48, 7.31–7.29 (1H each, ArH), 5.80 (1H each, vinyl CH), 5.45 (1H, vinyl CH) and 1.95 (3H, CH_3).

PMAEFc

Poly-2-(methacrylolyoxy)ethyl ferrocenecarboxylate) (PMAEFc) was synthesized according to previously reported procedure [1]. MAEFc (2.00 g, 5.84 mmol), AIBN (0.47 mg, 0.0058 mmol) and DDMAT (10 mg, 0.0292 mmol) were dissolved in DMF (1.2 mL). The reaction mixture was heated at 80 °C for 8 h, and then it was quenched by liq. nitrogen at a monomer conversion rate of 54%. The reaction mixture was dispersed in methanol (250 mL). The precipitates were filtered, centrifuged and dried in vacuum oven to obtain a yellowish solid (molecular weight determined by gel permeation chromatography (GPC)) Mn = 7.89×10^3 g/mol with PDI = 1.5. ^{1}H NMR (600 MHz, DMSO) δ ppm: 4.75 (2H, Cp), 4.5 (4H, OCH_2CH_2O), 4.40 (2H, Cp), 4.20 (5H, Cp) and 0.99–2.10 (CH_2 and CH_3).

Kinetic study of polymerization for MAEFc

Kinetic study was performed by following the reported procedure [1]. For example, HEMA (800 mg, 2.34 mmol), AIBN (1.76 mg, 0.009 mmol) and DDMAT (8.36 mg, 0.035 mmol) were dissolved in DMF (1.2 mL). The reaction mixture was refluxed for 8 h. Samples were taken out from the reaction mixture at different time intervals under the protection of Ar, and reaction was quenched by using liq. nitrogen. GPC and ^{1}H NMR techniques were used to study the conversion of monomer.

Synthesis of PMAEFc-*b*-PMVAPBA

Diblock copolymer (PMAEFc-*b*-PMVAPBA) was synthesized by using DDMAT as chain transferring agent, PMAEFc (ferrocene-containing homopolymer) was used as a macroinitiator and MVAPBA as boronic acid containing monomer. A typical polymerization procedure was as follows: PMAEFc (15 mg, 0.0438 mmol) and AIBN (1 mg, 0.008 mmol) were dissolved in DMF (1.0 mL) placed in a 20-mL reaction tube purged with Ar gas for 30 min. Under the protection of Ar gas, MVAPBA (1.798 g, 8.76 mmol) was added into the flask and polymerized at 80 °C for 8 h. The final diblock copolymer was obtained by precipitation in methanol (250 mL) and dried in open air and followed by drying in vacuum oven to obtain yellow brownish solid (molecular weight was determined by GPC) Mn = 1.92×10^5 g/mol with PDI = 1.5. ^{1}H NMR (600 MHz, DMSO)δ ppm: 8.10 (1H, NH), 7.90 (2H, (B(OH)2), 7.10–7.85 (4H, ArH), 4.75

Scheme 1 Synthesis of methyl vinylamino phenylboronic acid

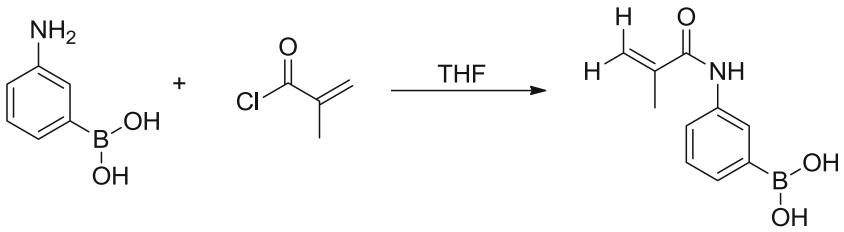

(2H, OCH_2CH_2O), 4.30 (2H, OCH_2CH_2O), 4.20–4.15 (9H, Cp), 2.99 (CH_2C), 2.10–1.90 (CH_2) and 0.90–1.35 (CH_3).

Micellization of PMAEFc-*b*-PMVAPBA

The procedure for constructing the micelles was as follows: PMAEFc-*b*-PMVAPBA (2.5 mg) was dissolved in 1 mL of THF followed by dropwise addition in deionized water (15 mL) with vigorous stirring. The solution was sonicated at room temperature for 30 min. The resulting solution was dialyzed using a semipermeable membrane (cut-off molecular weight 3500) against distilled water for 48 h to remove THF. The substantial removal of THF decreased solubility of hydrophobic part (ferrocene) to form the core and corona of PMAEFc-*b*-PMVAPBA micelles.

Glucose binding of PMAEFc-b-PMVAPBA micelles

Glucose powder (1 mg) and PMAEFc-*b*-PMVAPBA block copolymer (2.5 mg) were dissolved in THF (1 mL), and then the resulting solution was added dropwise in deionized water (10 mL) in about 30 min stirring. THF was removed by dialysis (cut-off molecular weight of semipermeable membrane was 3500) against deionized water for 48 h, and water was replaced every 5 h to ensure the full removal of excess amount of glucose (which failed to bind with BA).

Redox reactions of PMAEFc-b-PMAVPBA micelles

The well-dispersed micelles solution was treated with slight excess amount of $(NH_4)_2Ce(NO_3)_6$ compared to total ferrocene units present in PMAEFc-*b*-PMAVPBA, and the resultant solution was slowly stirred until yellow colour of the micelles changed into green. Subsequently, $NaHSO_3$ was introduced to the dispersion of oxidized micelles, and obtained solution was stirred until the colour was recovered back to yellow.

Characterization

Transmission electron microscope (TEM) images were obtained from JEOL model 1200EX microscope operated at 160 kV. ^{1}H NMR was measured using a 600 MHz AVANCE NMR spectrometer (Model DMX400). The chemical shifts were relative to tetramethylsilane (TMS) at δ = 0 ppm. Mw determination of homopolymer and block copolymer was performed by GPC (Waters Company, Model 2515-2414) with laser refractive index detector with Ultrastyral del column (pore size 103 to 105 Å). The mobile

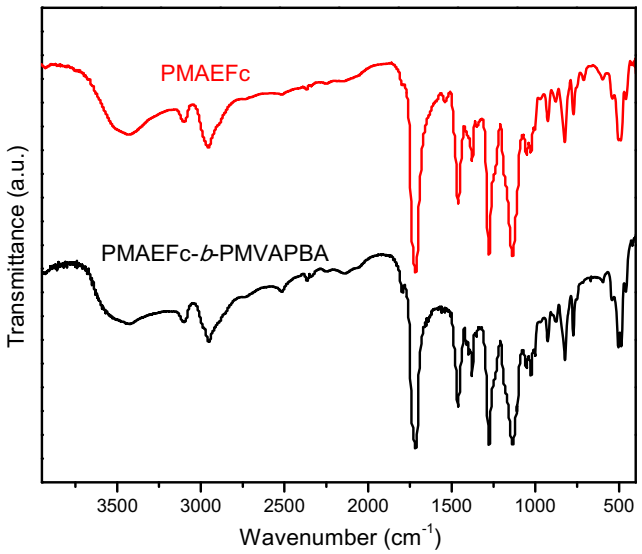

Fig. 1 FTIR spectra of *PMAEFc* and *PMAEFc-b-PMVAPBA*

Table 1 FTIR data of PMAEFc and PMAEFc-*b*-PMVAPBA [24, 25]

Functional group	Wavenumber (/cm)	
	PMAEFc	PMAEFc-*b*-PMVAPBA
OH	3423 (*b*)	3430 (*b*)
NH	3097 (*m*)	3101 (*w*)
C=O	1716 (*s*)	1717 (*s*)
C=C	1376 (*m*)	1378 (*m*)
	1460 (*m*)	1460 (*sh*)
B–O	1275 (*sh*)	1277 (*sh*)
C–H	773 (*m*)	772 (*sh*)
Ferrocene	503 (*m*)	489 (*m*)
	823 (*w*)	825 (*w*)
	1025 (*m*)	1027 (*w*)

Peak intensity: broad (*b*), medium (*m*), strong (*s*), sharp (*sh*) and weak (*w*)

Scheme 2 Synthesis of ferrocene boronic acid-based amphiphilic diblock copolymer by RAFT

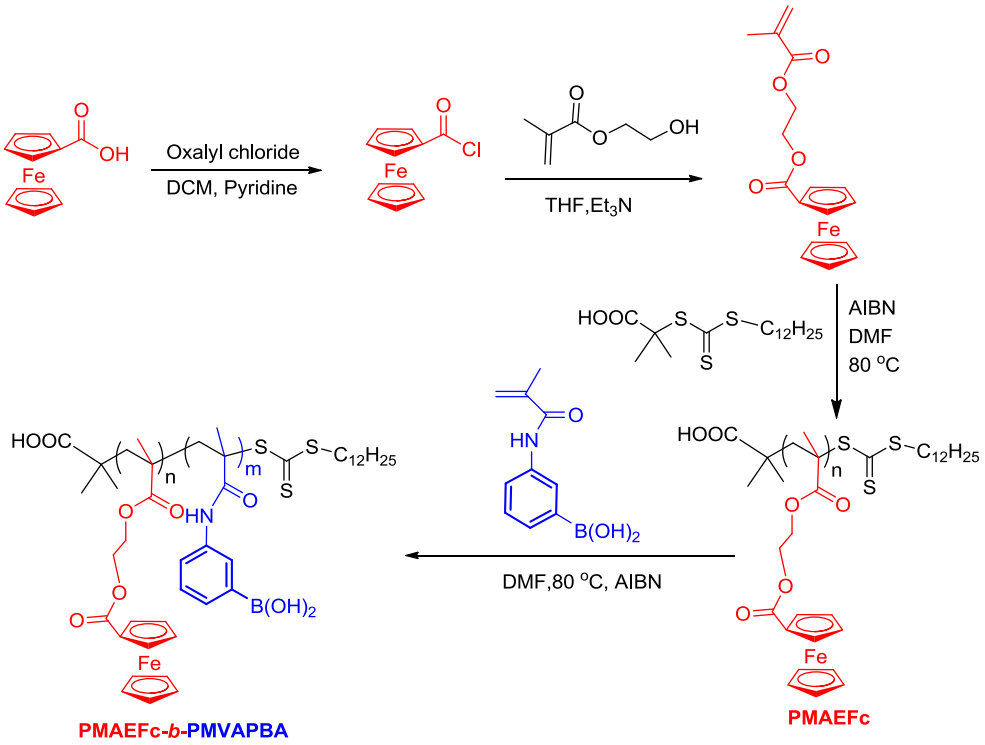

phase was 0.5 M solution of $NaNO_3$ in dimethylformamide (DMF) at 30 °C. Molecular weights were determined versus narrow distributed PMMA standards at a flow rate of 1.0 mL/min. The samples were prepared by dissolving 2 mg of corresponding polymer in 1 mL of DMF. Hydrodynamic diameter and zeta potential measurement were performed on Zetasizer

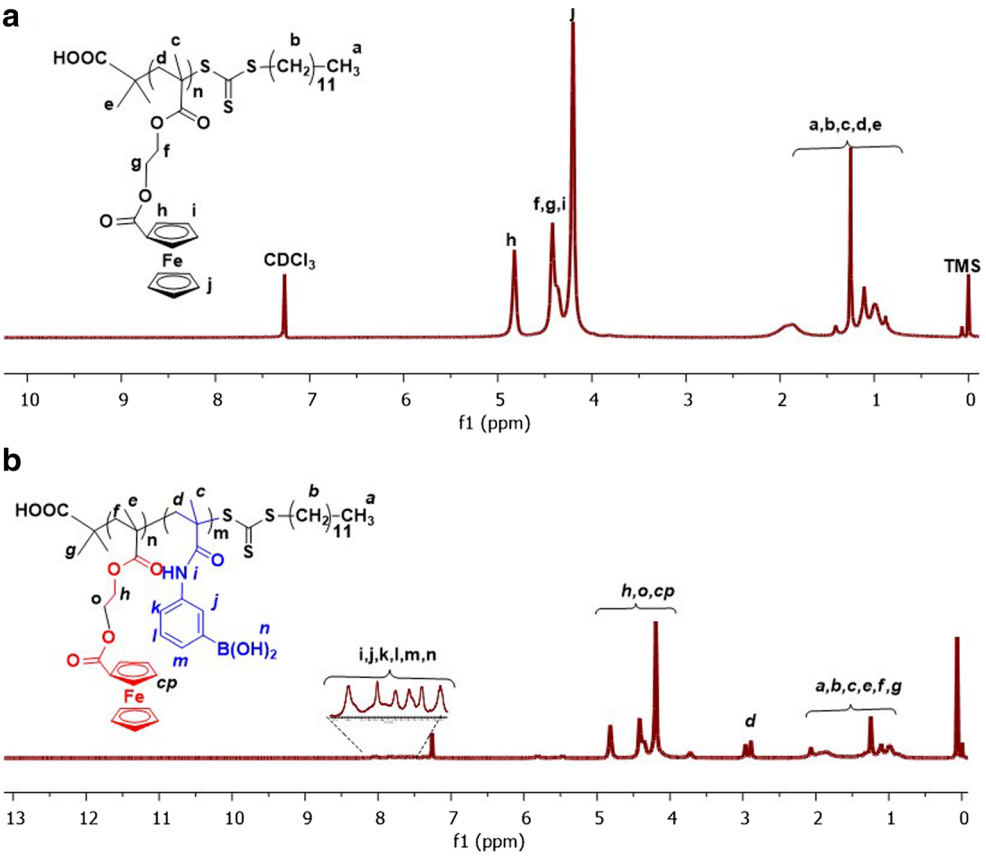

Fig. 2 NMR spectra. **a** PMAEFc. **b** PMAEFc-*b*-PMVAPBA

Table 2 GPC data of PMAEFc and PMAEFc-*b*-PMVAPBA

Sample	Mn (g/mol)	Mw (g/mol)	PDI
PMAEFc	7.89×10^3	1.21×10^4	1.5
PMAEFc-*b*-PMVAPBA	1.92×10^5	2.92×10^5	1.5

3000HSA. X-ray analysis was performed on XPert PRO (Cu K = 1.54 Å).

Results and discussion

Synthesis of MVAPBA and MAEFc and their RAFT polymerization

Methyl vinylamino phenylboronic acid (MVAPBA) was synthesized according to previously published report (Scheme 1) [22]. In FTIR spectra, PMAEFc and PMAEFc-*b*-PMVAPBA both showed characteristics amide peaks around 1750 and 1730/cm asymmetric C=O stretching vibrations [23]. N–H stretching vibrations (3150–3120/cm) also supported amide presence in derivatives. Hydroxyl absorption bands of boronic acids were appeared at 3550 and 3480/cm, while significant absorption peaks for B–O bond stretching were observed at 1385 and 1350/cm. Vibrational bands of ferrocenyl rings at 980, 820 and 500/cm were observed (Fig. 1; Table 1) [24].

RAFT polymerization was used to prepare ferrocene-containing homopolymer (PMAEFc) from MAEFc. The polymerization was performed at 80 °C using hydrophilic DDMAT as a chain transfer agent (Scheme 2). In ^{1}H NMR spectrum of PMAEFc, the vanishing of the vinyl protons of the methacrylate and appearance of new peaks at 0.90–1.05 and 1.75–2.10 ppm confirmed the successful polymerization (Fig. 2a).

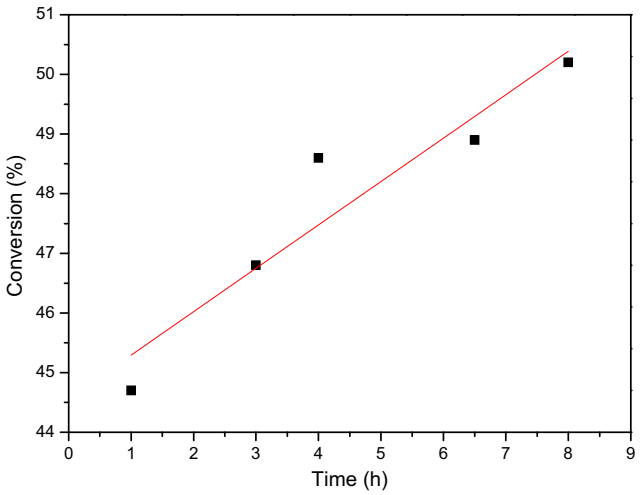

Fig. 3 A plot of MAEFc conducted via RAFT polymerization

PMAEFc-*b*-PMVAPBA was prepared using PMAEFc as a macroinitiator. MVAPBA as boronic acid containing monomer was used to prepare diblock polymer by chain extension with PMAEFc. Polymerization was performed in DMF with molar ratio PMAEFc/AIBN/monomer 1:0.2:200. Block copolymer, poly(2-(methacryloloyoxy)ethyl ferrocenecarboxylate-*b*-polymethyl vinylphenyl boronic acid (PMAEFc-*b*-PMVAPBA), was successfully synthesized (Scheme 2). In ^{1}H NMR spectrum, vanishing of vinyl protons at 5.70 and 6.20 ppm and the increase in the intensity of the signals at 0.9–1.10 and 1.80–2.0 ppm indicated that MVAPBA was successfully polymerized (Fig. 2b). GPC results (Table 2) also confirmed the chain extension of PMAEFc-*b*-PMVAPBA.

Kinetic study was performed to examine RAFT polymerization of MAEFc. The conversion rate was monitored by matching peak area of vinyl proton at 5.70 ppm with peaks area of Cp rings at 4.20–4.40 ppm. The plot (Fig. 3) showed a linear relationship between conversion rate and reaction time, which indicated that the RAFT polymerization displayed a controlled living character.

After 8 h, 50.2% conversion of monomer was achieved. GPC data is shown in Table 3, which is also in agreement with ^{1}H NMR results that polymerization followed a controlled character.

Micellization of PMAEFc-*b*-PMAVPBA

The block copolymer micellization in selective solvent system is a typical feature of its colloidal properties. When the block copolymer is dissolved in a solvent, which is thermodynamically good for one block and a precipitant for the other, then copolymer chains may assemble reversibly to form micellar aggregates. The micelle consists of a more or less swollen core of the insoluble blocks, which is surrounded by a flexible fringe of soluble blocks. Such micelles are usually spherical with narrow size distribution and may change in their size distribution and shape under certain conditions [20, 26]. In this study, we have investigated the micellization of block copolymer by two different methods. The typical procedure of first method was to dissolve PMAEFc-*b*-PMVAPBA in THF and dialyze it in water for 2 days at 15 °C. In second method, binary mixture of suitable solvents with different volume ratio was mixed and appropriate amount of PMAEFc-*b*-PMVAPBA was dissolved to form micelles [1]. The synthesized amphiphilic block copolymer (PMAEFc-*b*-PMAVPBA) containing ferrocene and boronic acid as hydrophobic blocks was expected to form micelles by self-assembling into aqueous solution. Therefore, micelle preparation was endeavored by dissolving PMAEFc-*b*-PMAVPBA in THF, followed by the addition of the THF solution into water. On water addition,

Table 3 Monomer conversion of PMAEFc

Sample	Polymerization (h)	% Conversion (^{1}H NMR)	Mw (GPC)
PMAEFc-8 h	8	50.2	1.21×10^4
PMAEFc-6.5 h	6.5	48.9	8.82×10^3
PMAEFc-4 h	4	48.6	7.56×10^3
PMAEFc-3 h	3	46.8	7.44×10^3
PMAEFc-1 h	1	44.7	7.38×10^3

resulting solution turned from wholly transparent to slightly turbid, showing the micelles formation. THF was completely removed by dialysis, and finally, aqueous micellar solutions were obtained. The micelle morphology was observed by TEM. Figure 4 shows the SEM images, and Fig. 5 shows TEM images of typical micelles obtained from PMAEFc-*b*-PMAVPBA.

TEM images showed spherical micelles with size about 134–172 nm. DLS was employed to measure the hydrodynamic radii (R_h) of the micelles. Well-defined micelles with spherical morphology were successfully prepared by using amphiphilic PMAEFc-*b*-PMVAPBA with size in the range of 530–721 nm.

Glucose binding of PMAEFc-*b*-PMVAPBA micelles

In order to investigate glucose binding of ferrocene boron containing block copolymer, PMAEFc-*b*-PMVAPBA and glucose were mixed together in equimolar ratio (number of boronic acid blocks and glucose molecules) and employed to bind. The solution was further dialyzed to form micelles and to remove unbound glucose molecules.

The binding of glucose with boronic acids hydroxyls was confirmed by TEM and DLS studies. Due to binding of glucose with boronic acid hydroxyls, hydrophilic part of micelles was increased and micelles disintegrated (disturbed the ratio of hydrophobic and hydrophilic part, which led to core and corona undistinguishable) into separate blocks, resulting in low aggregation and decrease in size (R_h = 105 nm) as compared to unbound micelles of PMAEFc-*b*-PMVAPBA (R_h = ~550 nm) (Fig. 6). This phenomenon can also be explained as the reduction in size due to the transition of the block copolymer from amphiphilic (where itself assembles to form micelles) to completely hydrophilic (where it would exists as unimers) after binding of the glucose to the boronic acid units. Essentially, esterification of the boronic acid moieties with the glucose led to the boronic acid block becoming hydrophilic.

These results are in agreement with the reported literature, except the size of unimers, which was a little larger. Reason might be due to significant aggregation caused by the oxidation of ferrocene to ferrocenium within the system. In addition to DLS results, disconnection was also clear by visual examination, as yellowish and slightly turbid aggregate solution of PMAEFc-*b*-PMVAPBA instantly became transparent on addition of glucose. Such phenomenon was possibly ascribed to the mostly hydrophobic/neutral boronic acid group transformation into aggregates after converting to hydrophilic/anionic cyclic boronates upon binding with glucose. Thus, it disturbs hydrophilicity of boronic acid and disintegrates it into smaller parts [27].

Effect of redox-responsive ferrocene on the morphology of PMAEFc-*b*-PMVAPBA micelles

The spherical micelles consist of ferrocene conjugated PMAEFc blocks as core and soluble boronic acid blocks as corona. The size of the micelles could be triggered via

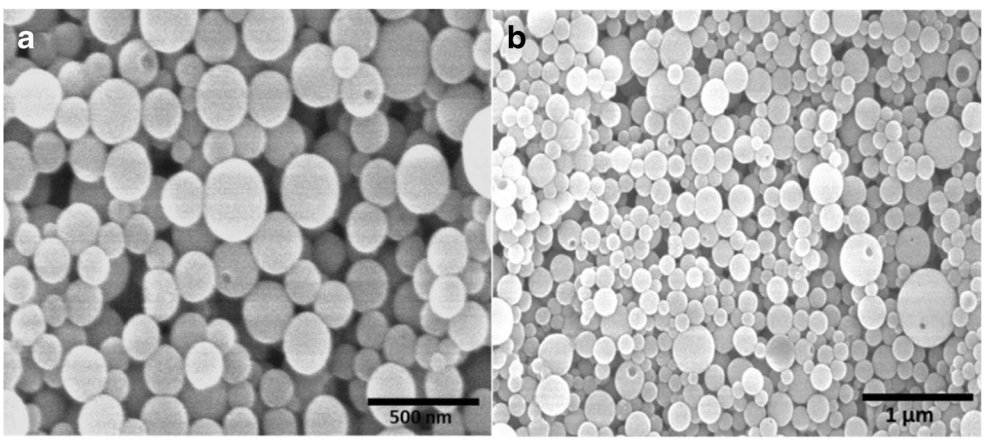

Fig. 4 SEM images of PMAEFc-*b*-PMVAPBA spherical micelles obtained via dialysis in aqueous solution

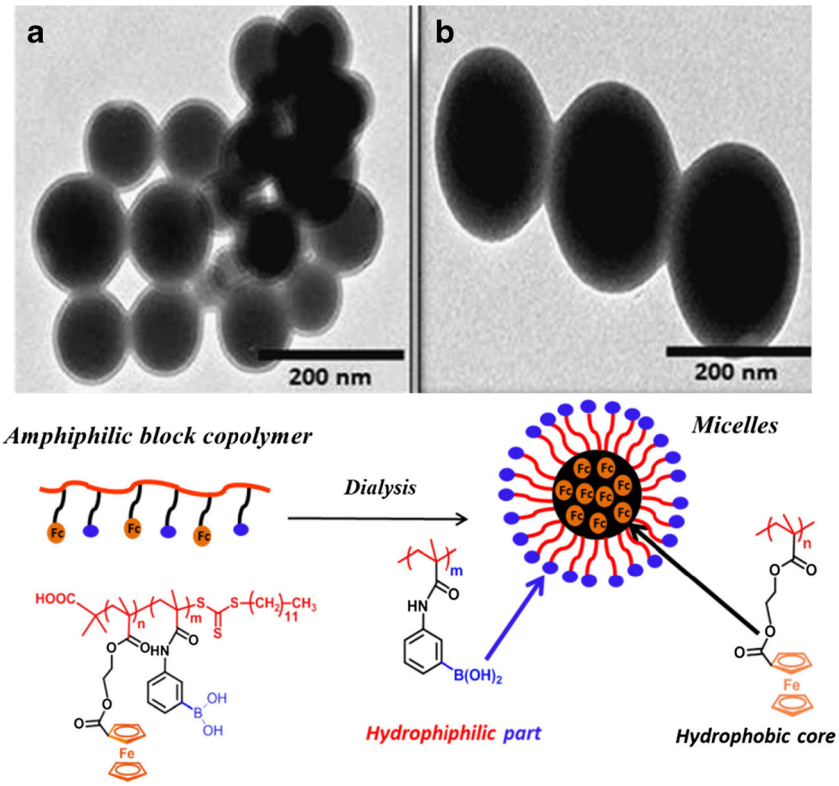

Fig. 5 TEM images of PMAEFc-*b*-PMVAPBA spherical micelles showing core and corona of ferrocene and boronic acid part respectively,along with possible graphical representation

chemical stimuli, i.e. altering the redox state of ferrocene due to redox reactions. The reversible redox reactions of PMAEFc-*b*-PMAVPBA micelles were performed using $(NH_4)_2Ce(NO_3)_6$ and $NaHSO_3$ as oxidizing and reducing agents, respectively. However, the ferrocene containing block copolymer showed change in their sizes due to the redox reactions, as demonstrated by the measurements of TEM (Fig. 7). Oxidation of micelles by $(NH_4)_2Ce(NO_3)_6$ increased the size of micelles (see Table 4 for details). Such variation in size was attributed to the conversion of ferrocene (neutral) moiety to ferrocenium (positively charged) after oxidation reaction in the core.

The electrostatic repulsive interactions between the positively charged ferrocene blocks resulted into an incompact core and apparently larger size of micelles. Upon reduction by $NaHSO_3$, the micelles were recovered to almost their original size. These findings showed that PMAEFc-*b*-PMAVPBA micelles experienced a reversible redox-triggered change in their size. It is important to mention here that the size of micelles of PMAEFc-*b*-PMAVPBA examined by DLS (~530 nm; Fig. 7) was much larger than that determined by TEM image (~150 nm; Fig. 7). It has been well established that diameter of block copolymer micelles determined by TEM is typically smaller than those determined by DLS.

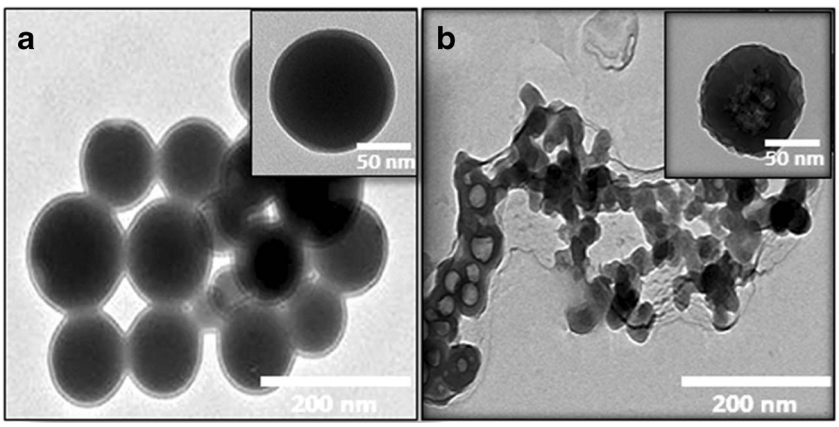

Fig. 6 TEM images. **a** PMAEFc-*b*-PMVAPBA. **b** PMAEFc-*b*-PMVAPBA + glucose

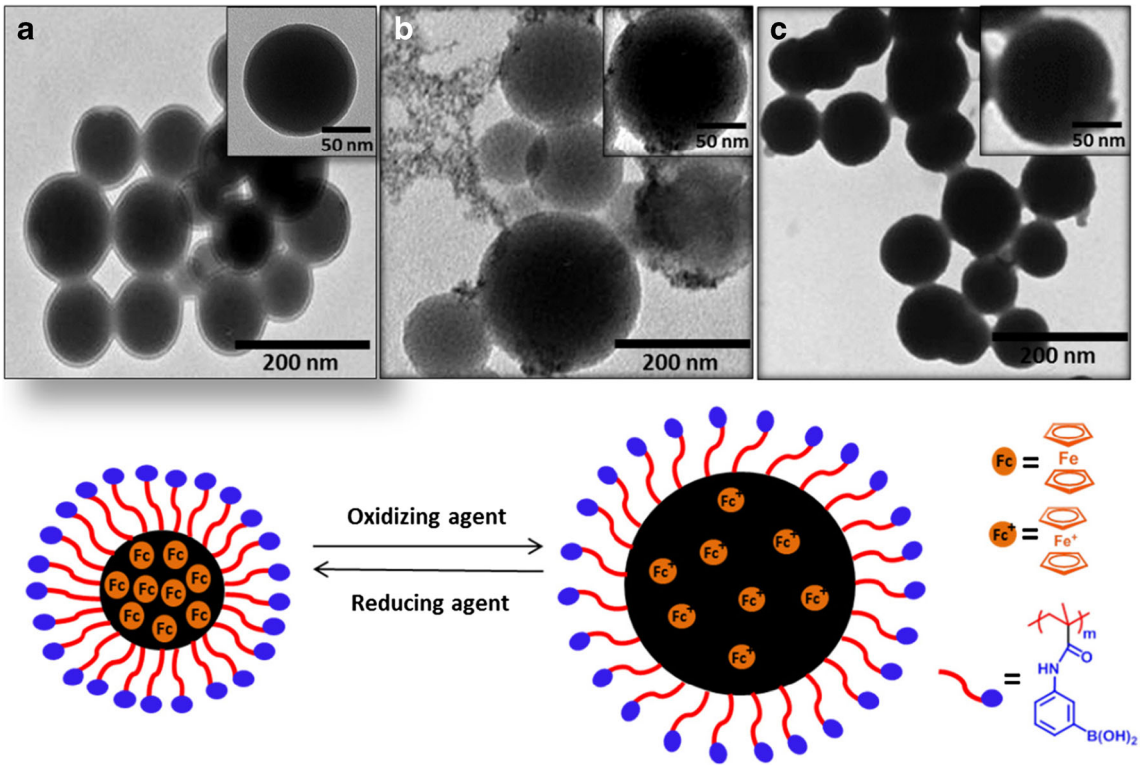

Fig. 7 TEM images of **a** pure sample PMAEFc-*b*-PMVAPBA, **b** oxidized PMAEFc-*b*-PMVAPBA and **c** reduced PMAEFc-*b*-PMVAPBA, along with the possible mechanism

The more convincing explanations for such difference are as follows: Firstly, TEM images reflect conformations in the dry state, while DLS involves the dimension of both stretched shell and the swollen core. It can also be described as reduction of the droplet by water evaporation during the sample preparation on copper-coated grid of TEM. Secondly, only the core of the micelles could be detected by TEM due to not enough chain density in the corona to make visible contrast to the background [20, 28]. Therefore, it is very likely that the observed size of aggregates by DLS is larger than the expected from TEM. The zeta potentials of pure-PMAEFc-*b*-PMAVPBA, oxidized-PMAEFc-*b*-PMAVPBA and reduced-PMAEFc-*b*-PMAVPBA were −18.8, 33 and −13.8 mV, respectively as shown in Table 4.

In pure form of PMAEFc-*b*-PMAVPBA, negative charge was attributed to charged phenylboronic acid (PBA) moieties present in the solution, while oxidation of ferrocene (neutral) resulted in the formation of ferrocenium (positively charged); thus, it balanced the negative charge of PBA and increased the positive charge of the micelle. In case of reduced form of PMAEFc-*b*-PMAVPBA, ferrocenium was reduced to ferrocene and the overall apparent zeta potential was due to negatively charged PBA.

Thermal properties of PMAEFc and PMAEFc-*b*-PMVAPBA

Differential scanning calorimetry (DSC) and thermal gravimetric analysis (TGA) were performed to investigate the thermal properties of ferrocene-based homopolymer and blocked copolymers (Fig. 8). The glass transition temperature (T_g) of PMAEFc was 57 °C, while PMAEFc-*b*-PMVAPBA exhibited comparatively higher T_g (77 °C). The difference in T_g of block copolymer was mainly due to the incorporation of second

Table 4 Diameter observed by TEM and DLS with a concentration of 0.05 mg/L of PMAEFc-*b*-PMAVPBA

Sample	Zeta potential (mV)[a]	D_h (nm)[a]	D_{TEM} (nm)[b]
PMAEFc-*b*-PMAVPBA (pure)	−18.8	530 ± 20.2	134 ± 35
PMAEFc-*b*-PMAVPBA (oxidized)	33	1465 ± 14.9	238 ± 35
PMAEFc-*b*-PMAVPBA (reduced)	−13.8	721 ± 14.0	172 ± 20

[a] Data from DLS

[b] Data from TEM

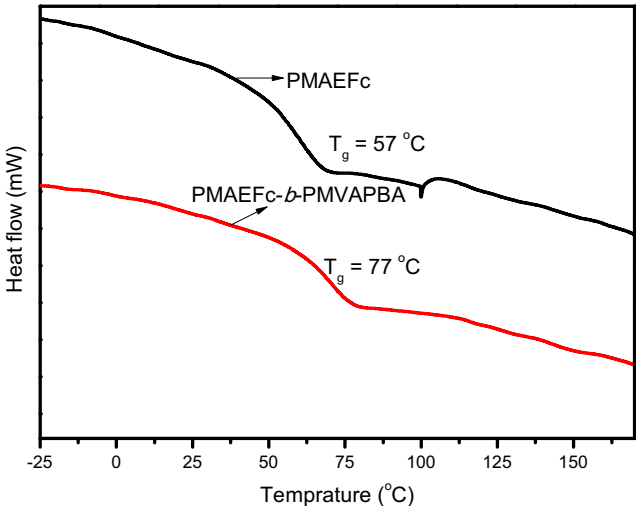

Fig. 8 DSC curves of PMAEFc and PMAEFc-*b*-PMVAPBA

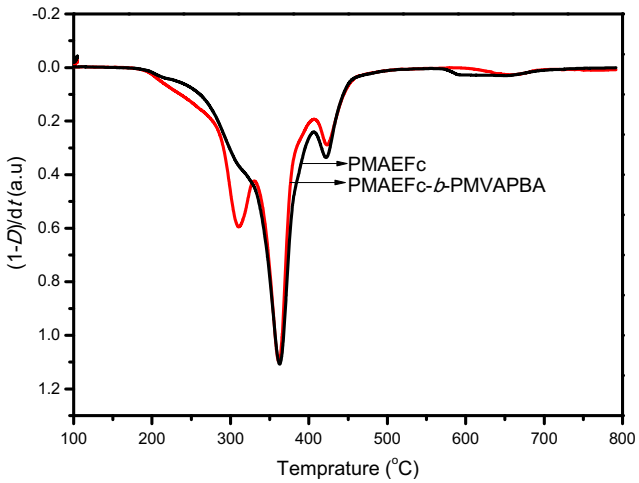

Fig. 10 DTG curves of PMAEFc and PMAEFc-*b*-PMVAPBA

block and higher molecular weight of copolymer than homopolymer. It was observed that weight loss in homopolymer and block copolymers occurred in three-steps (Figs. 9 and 10). The first stage of weight loss appeared in the range of 250–325 °C due to the degradation of the aliphatic groups (ester C=O and C–O bonds) connected to the ferrocene units into a large amount of carbon dioxide [29–31].

The aryl boronic acid moieties and Fe–C bonds were broken at 450 °C, which constitute second stage of weight loss. The release of iron (Fe) atoms can catalyze the degradation of the polymer due to its good catalytic effect. The small weight loss in the third stage represented the degradation of the ferrocene units present in the polymer. The weight loss stopped after 500 °C, and the main components of the residue (14.72–15.60%) were carbon and iron.

The temperature of 5% weight loss (T_5), the temperature of 10% weight loss (T_{10}) and the char yields of polymers were obtained from TGA curves recorded at heating rate of 20 °C/min under nitrogen atmosphere (Table 5).

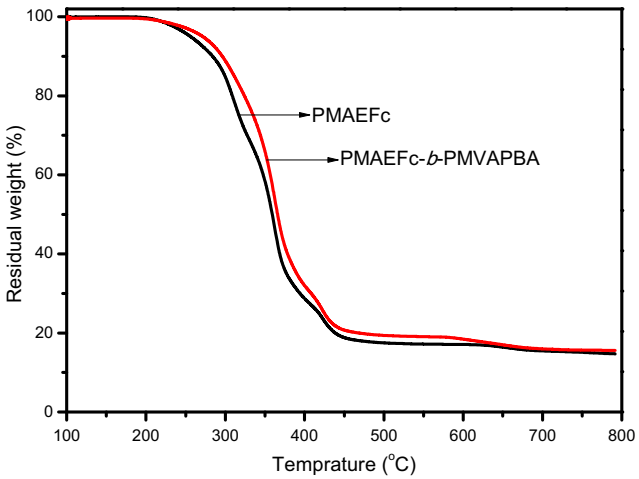

Fig. 9 TGA curves of PMAEFc and PMAEFc-*b*-PMVAPBA

X-ray diffraction studies of PMAEFc and PMAEFc-*b*-PMVAPBA

The crystallinity and chain packing of the homopolymer (PMAEFc) and block copolymer (PMAEFC-*b*-PMVAPBA) were analyzed by powder X-ray diffraction in the region of 2θ = 5–80° at room temperature. Regardless of the molecular weights, the XRD patterns of both homo and block polymers were broad without obvious peak features, indicating their amorphous nature (Fig. 11). This amorphous nature of the polymer is also reflected in its good solubility in THF, DMF and DMSO.

The amorphous nature of the polymers could be attributed to the introduction of pendant alkyl chain and bulky ferrocene group in the polymer chain, which resulted the poor intermolecular packing. The mean intermolecular distances (*d*-spacing) of these polymers could be also calculated from the maxima of the broad diffraction peaks by Bragg's equation.

$$2d\mathrm{Sin}\theta = n\lambda$$

PMAEFc exhibited the diffraction peak at 2θ = 16.3° with *d*-spacing of 0.81 Å, whereas PMAEFc-*b*-PMVAPBA

Table 5 Thermal properties of PMAEFc and PMAEFc-*b*-PMVAPBA

Polymer	T_g	T_5	T_{10}	Char yield at 800 °C (%)
PMAEFc	57	256	284	14.72
PMAEFc-*b*-PMVAPBA	77	271	296	15.60

T_g, obtained from DSC as baseline shift in the second heating scan at a heating rate of 10 °C/min under nitrogen atmosphere; T_5, temperature at which 5% weight loss was recorded by TGA at a heating rate of 20 °C/min under nitrogen atmosphere; T_{10}, temperature at which 10% weight loss was recorded by TGA at a heating rate of 20 °C/min in nitrogen, char yield and residual weight retention under N_2 atmosphere at 800 °C

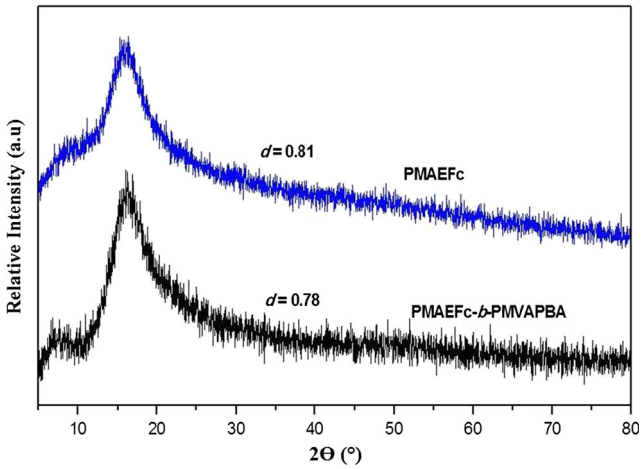

Fig. 11 Powder X-ray diffractograms of PMAEFc and PMAEFc-*b*-PMVAPBA

demonstrated diffraction peak at $2\theta = 15.9°$ with *d*-spacing of 0.78 Å. In comparison, it could be observed that the *d*-spacing of PMAEFc-*b*-PMVAPBA is smaller than PMAEFc, which could be attributed to the intermolecular interactions among phenyl boronic acid groups into block copolymer resulting offered tight chain packing and greater aggregation. XRD results are consistent with other findings from T_g.

Conclusion

1) Ferrocene-based block copolymer (PMAEFc-*b*-PMVAPBA) by using 2-(dodecylthio–carbono-thioylthio)-2-methyl propanoic acid (DDMAT) as RAFT agent was synthesized. PMAEFc-*b*-PMVAPBA was linked to hydrophobic blocks of methyl vinylamino phenylboronic acid and ferrocene (redox-active). PMAEFc-*b*-PMVAPBA was characterized by FTIR, ^{1}H NMR and GPC. The thermal properties of PMAEFc and PMAEFc-*b*-PMVAPBA were studied by using thermal gravimetric analysis (TGA) and differential scanning calorimetry (DSC). The hydrophobic and hydrophilic blocks of copolymer self-assembled into spherical micelles in aqueous solution. The redox behaviour of ferrocene was studied by using water-soluble $(NH_4)_2Ce(NO_3)_6$ and $(NaHSO_3)$ as oxidizing and reducing agents, respectively. Dynamic light scattering (DLS) and transmission electron microscopy (TEM) were used to investigate the redox-controlled behaviour of micelles.
2) It was found that the change in polarity and swelling of micelles increased the hydrodynamic diameter due to the oxidation of ferrocene and glucose binding with boronic acid hydroxyls led to less aggregates or unimers. The redox-responsive behaviour provides a criterion for detection/binding of biological analytes study and redox-controlled release of encapsulants. Overall, the synthesis and the binding of glucose with boronic acids both can demonstrate an example of saccharide sensing, which can be utilized to construct redox-responsive saccharide detection sensors.

Acknowledgements Financial supports from the National Natural Science Foundation of China (51673170, 21472168, 21372200 and 21272210), the Science and Technology Innovation Team of Ningbo (2011B82002) and the Fundamental Research Funds for the Central Universities (2016FZA4018) are gratefully acknowledged.

Compliance with ethical standards

Conflict of interest The authors declare that they have no conflict of interest.

References

1. Zhang JY, Ren LX, Hardy CG, Tang CB (2012) Cobaltocenium-containing methacrylate homopolymers, block copolymers, and heterobimetallic polymers via RAFT polymerization. Macromolecules 45(17):6857–6863
2. Ren L, Hardy CG, Tang S, Doxie DB, Hamidi N, Tang C (2010) Preparation of side-chain 18-e cobaltocenium-containing acrylate monomers and polymers. Macromolecules 43(22):9304–9310
3. Nagaki A, Miyazaki A, Yoshida J-i (2010) Synthesis of polystyrenes-poly(alkyl methacrylates) block copolymers via anionic polymerization using an integrated flow microreactor system. Macromolecules 43(20):8424–8429
4. Ye X, Niroomand H, Hu S, Khomami B (2015) Block copolymer micelle formation in a solvent good for all the blocks. Colloid Polym Sci 293(10):2799–2805
5. Yang F, Cao Z, Wang G (2015) Micellar assembly of a photo- and temperature-responsive amphiphilic block copolymer for controlled release. Polym Chem 6(46):7995–8002
6. Schmidt BVKJ, Elbert J, Barner-Kowollik C, Gallei M (2014) Individually addressable thermo- and redox-responsive block copolymers by combining anionic polymerization and RAFT protocols. Macromol Rapid Comm 35(7):708–714
7. Schattling P, Jochum FD, Theato P (2014) Multi-stimuli responsive polymers—the all-in-one talents. Polym Chem 5(1):25–36
8. Morsbach J, Natalello A, Elbert J, Winzen S, Kroeger A, Frey H, Gallei M (2013) Redox-responsive block copolymers: poly(vinylferrocene)-b-poly(lactide) diblock and Miktoarm star polymers and their behavior in solution. Organometallics 32(20):6033–6039
9. Liu L, Rui L, Gao Y, Zhang W (2015) Self-assembly and disassembly of a redox-responsive ferrocene-containing amphiphilic block copolymer for controlled release. Polym Chem 6(10):1817–1829
10. Chang X, Dong R, Ren B, Cheng Z, Peng J, Tong Z (2014) Novel ferrocenyl-terminated linear-dendritic amphiphilic block copolymers: synthesis, redox-controlled reversible self-assembly, and oxidation-controlled release. Langmuir 30(29):8707–8716
11. Janczewski D, Song J, Csanyi E, Kiss L, Blazso P, Katona RL, Deli MA, Gros G, Xu J, Vancso GJ (2012) Organometallic polymeric carriers for redox triggered release of molecular payloads. J Mater Chem 22(13):6429–6435
12. Eloi J-C, Rider DA, Cambridge G, Whittell GR, Winnik MA, Manners I (2011) Stimulus-responsive self-assembly: reversible, redox-controlled micellization of polyferrocenylsilane diblock copolymers. J. Amer. Chem. Soc. 133(23):8903–8913

13. Wang JS, Matyjaszewski K (1995) Controlled living radical polymerization-atom-transfer radical polymerization in the presence of transition-metal complexes. J Amer Chem Soc 117(20): 5614–5615
14. Moad G (2015) RAFT (reversible addition-fragmentation chain transfer) crosslinking (co)polymerization of multi-olefinic monomers to form polymer networks. Polym Int 64(1):15–24
15. Fortin N, Klok HA (2015) Glucose monitoring using a polymer brush modified polypropylene hollow fiber-based hydraulic flow sensor. ACS Appl Mater Interfaces 7(8):4631–4640
16. Cheng F, Wan W-M, Zhou Y, Sun X-L, Bonder EM, Jäkle F (2015) Borinic acid block copolymers: new building blocks for supramolecular assembly and sensory applications. Polym Chem 6(25): 4650–4656
17. Takara M, Toyoshima M, Seto H, Hoshino Y, Miura Y (2014) Polymer-modified gold nanoparticles via RAFT polymerization: a detailed study for a biosensing application. Polym Chem 5(3):931–939
18. Ciftci H, Tamer U, Sen Teker M, Pekmez NO (2013) An enzyme free potentiometric detection of glucose based on a conducting polymer poly (3-aminophenyl boronic acid-co-3-octylthiophene). Electrochim Acta 90:358–365
19. Li Y, Xiao W, Xiao K, Berti L, Luo J, Tseng HP, Fung G, Lam KS (2012) Well-defined, reversible boronate crosslinked nanocarriers for targeted drug delivery in response to acidic pH values and cis-diols. Angew Chem Int Edit 51(12):2864–2869
20. Xiao Z-P, Cai Z-H, Liang H, Lu J (2010) Amphiphilic block copolymers with aldehyde and ferrocene-functionalized hydrophobic block and their redox-responsive micelles. J Mater Chem 20(38): 8375
21. Kim BY, Ratcliff EL, Armstrong NR, Kowalewski T, Pyun J (2010) Ferrocene functional polymer brushes on indium tin oxide via surface-initiated atom transfer radical polymerization. Langmuir 26(3):2083–2092
22. Roy D, Cambre JN, Sumerlin BS (2009) Triply-responsive boronic acid block copolymers: solution self-assembly induced by changes in temperature, pH, or sugar concentration. Chem Commun 16: 2106–2108
23. Hosseinzadeh R, Mohadjerani M, Pooryousef M, Eslami A, Emami S (2015) A new boronic acid fluorescent sensor based on fluorene for monosaccharides at physiological pH. Spectrochim Acta A Mol Biomol Spectrosc 144:53–60
24. Zain ul A, Wang L, Yu H, Saleem M, Akram M, Abbasi NM, Khalid H, Sun R, Chen Y (2016) Ferrocene-based polyethyleneimines for burning rate catalysts. N J Chem 40(4): 3155–3163
25. Zhang R, Miao J-P, Ge C-H, Zhang M-Y, Wang L-X, Zhang X-D (2014) Mono- and di-phenylboronic acid receptors with fluorescence sensitivity to d-fructose. Sensor Actuat B Chem 198:260–267
26. Riess G (2003) Micellization of block copolymers. Prog Polym Sci 28(7):1107–1170
27. Roy D, Sumerlin BS (2012) Glucose-sensitivity of boronic acid block copolymers at physiological pH. ACS Macro Lett 1(5): 529–532
28. Khan W, Seo J-M, Park S-Y (2011) Synthesis and micellization of a novel diblock copolymer of poly(N-isopropylacrylamide)-b-SGLCP and its application in stability of 5CB droplets in aqueous medium. Soft Matter 7(2):780–787
29. Derue L, Dautel O, Tournebize A, Drees M, Pan H, Berthumeyrie S, Pavageau B, Cloutet E, Chambon S, Hirsch L, Rivaton A, Hudhomme P, Facchetti A, Wantz G (2014) Thermal stabilisation of polymer–fullerene bulk heterojunction morphology for efficient photovoltaic solar cells. Adv Mater 26(33):5831–5838
30. Amer WA, Wang L, Amin AM, Yu H, Li C, Ma L (2013) Study on the electrochemical, thermal, and liquid crystalline properties of poly(diethyleneglycol 1,1′-ferrocene dicarboxylate). Des Monomers Polym 16(2):1–10
31. Patrícia SOP, Hállen DRC, Flávio ACdO, Ariete R, Bernardo RAN, Glaura GS, Luiz AC (2006) Correlation between thermal, optical and morphological properties of heterogeneous blends of poly(3-hexylthiophene) and thermoplastic polyurethane. J Phys-Condens Mat 18(32):7529